Walking mechanism of the intracellular cargo transporter myosin V

2006 J. Phys.: Condens. Matter 18 S1943

(http://iopscience.iop.org/0953-8984/18/33/S12)

INSTITUTE OF PHYSICS PUBLISHING JOURNAL OF PHYSICS: CONDENSED MATTER

J. Phys.: Condens. Matter **18** (2006) S1943–S1956 doi:10.1088/0953-8984/18/33/S12

Walking mechanism of the intracellular cargo transporter myosin V

Stephan Schmitz[1,3], **Jayne Smith-Palmer**[1], **Takeshi Sakamoto**[2], **James R Sellers**[2,3] **and Claudia Veigel**[1,3]

[1] Physical Biochemistry, National Institute for Medical Research, The Ridgeway, Mill Hill, London NW7 1AA, UK
[2] Laboratory of Molecular Physiology, National Heart, Lung and Blood Institute, NIH, Bethesda, MD 20892, USA

E-mail: sschmit@nimr.mrc.ac.uk, sellersj@nhlbi.nih.gov and cveigel@nimr.mrc.ac.uk

Received 3 February 2006, in final form 6 February 2006
Published 4 August 2006
Online at stacks.iop.org/JPhysCM/18/S1943

Abstract

Motor proteins of the myosin, kinesin and dynein families transport vesicles and other cargo along tracks of actin filaments or microtubules through the cytoplasm of cells. The mechanism by which myosin V, a motor involved in several types of intracellular transport, moves processively along actin filaments, has recently been the subject of many single molecule biophysical studies. Details of the molecular mechanisms by which this molecular motor operates are starting to emerge.

1. Introduction

Many types of cellular motility are driven by myosin motors interacting with actin filaments, producing force and movement coupled to the hydrolysis of ATP. Class V myosins transport cytoplasmic vesicles and organelles along actin filaments, the polarity of which determines the direction of movement. Mammalian myosin V is a homodimer of motor heads, each monomer formed by a motor domain followed by an α-helical neck region stabilized by six calmodulins (figure 1(A)). The molecule is dimerized by its coiled coil forming tail, and ends in a globular domain responsible for cargo binding. To ensure efficient translocation of their cargo over micrometre distances, organelle motors of the kinesin and myosin families are often processive, dimeric molecules that can take tens to hundreds of steps per diffusional encounter before dissociating from their filament track. Myosin V has evolved several molecular properties that enable it to function efficiently as an organelle motor. First, the coiled coil motif in the tail domain enables the motor to dimerize stably and form a two-headed molecule. Second, the ATPase cycle time of a single myosin V head is dominated by states with high affinity for actin, increasing the time during which the myosin V dimer remains attached to actin [1]. Third, the

[3] Authors to whom any correspondence should be addressed.

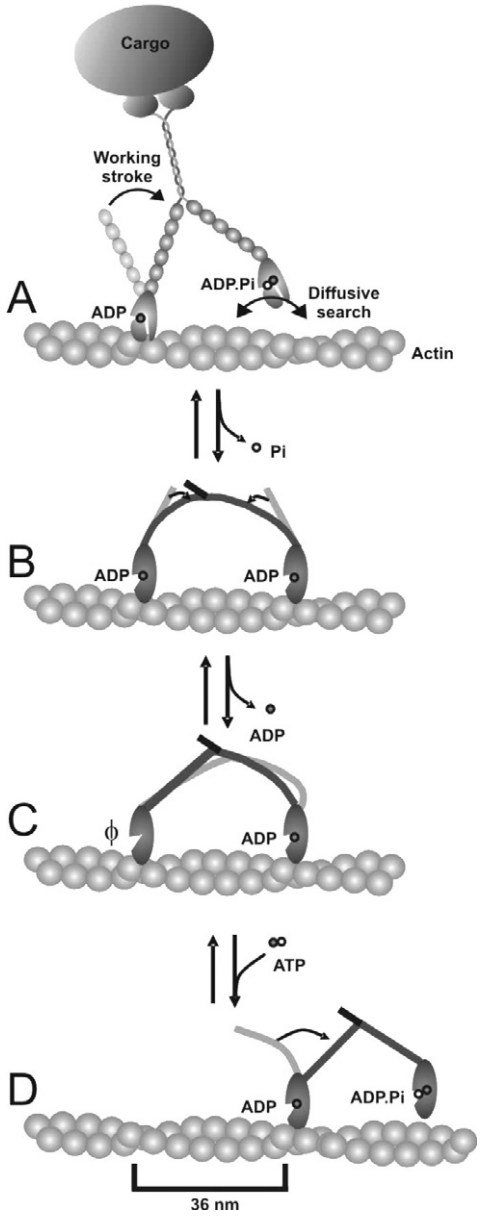

Figure 1. The cartoon illustrates structural features of a myosin V molecule and shows a model for processive movement of myosin V along the 36 nm helical repeat of actin. (A) One head attaches first and produces a working stroke of ∼20 nm, probably coupled to the release of phosphate. While ADP is still bound to this head, the unbound head explores the free energy landscape of the actin filament surface, driven by thermal motion. The working stroke of the first head has positioned the second head such that it experiences a diffusional force (derivative of the sinusoidal free energy landscape) directed towards the next preferred binding position [6]. (B) The second head binds, causing intramolecular strain (stored as an elastic strain energy). The elastic strain decelerates ADP release from the second head and accelerates the release of ADP from the first head. On the first head this is coupled to a second conformational change (∼5 nm), which relieves some of the internal strain. (C) Subsequent ATP binding will cause the first head to detach and (D) the second head to undergo its working stroke so that the next 36 nm step can be made.

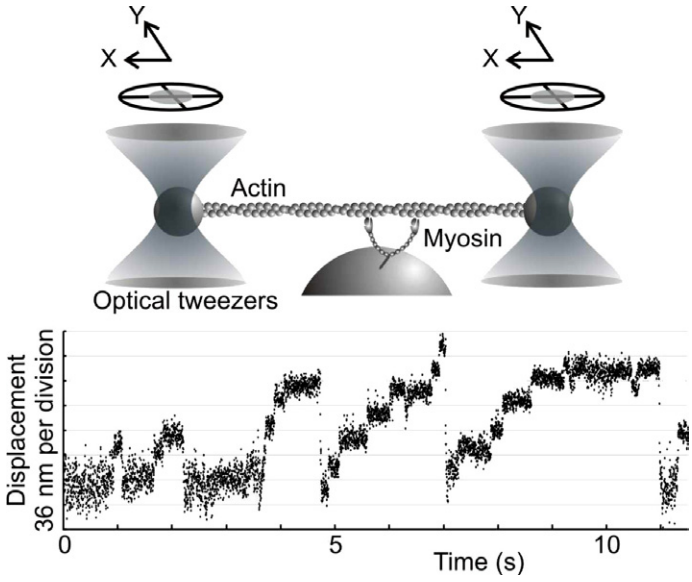

Figure 2. Single molecule mechanical interactions of myosin V measured using an optical tweezers based force transducer. Binding events with one to seven successive steps were observed (100 μM ATP). The cartoon shows a single myosin motor interacting with an actin filament suspended between two plastic beads held in two optical tweezers.

long neck domain enables myosin V to take 36 nm steps, a length equal to the pseudo-repeat distance of the helical actin filament. Thus, cargo can be transported to its destination along the shortest path along the longitudinal axes of actin filaments. This could be relevant in particular for transport along membrane-associated filaments, where myosin V taking its cargo on a spiral path around actin may quickly run into the membrane. Fourth, the globular tail domain of myosin V binds cargo reversibly via regulatory protein complexes [2–4]. Fifth, the motor can be inactivated by changing its conformation in a Ca^{2+} and cargo dependent manner [5].

The 36 nm step size of a processively moving dimeric myosin V molecule has been observed directly in single molecule mechanical (figure 2, [6–13]) and fluorescence studies [14–18] and is also consistent with electron microscopic images of myosin V molecules bound with both heads to actin in the presence of ATP [19]. Each 36 nm step appears to be produced by a combination of a working stroke of a single bound head, which rotates its neck region to move the centre of mass of the molecule forward by ∼20–25 nm [6, 20], and a thermal component produced by the free head undergoing a diffusional search for a new binding site along actin, which moves the centre of mass forward by another ∼11–16 nm [6] (figure 1(A)). Electron micrographs of myosin V molecules are consistent with the idea that the power stroke of the bound head positions the free head to explore binding sites preferably in the forward direction along the actin filament [19, 21]. The narrow distribution of step sizes seen in single molecule mechanical experiments and the relatively constant head–head distance observed in electron microscope images (13 ± 1 actin monomers apart) suggest that myosin V has a great preference for binding to the actin monomer which provides least azimuthal distortion when both heads are bound.

Solution kinetic studies of single headed myosin V constructs (MVS1) suggest that the acto-myosin V ATPase cycle is tuned for processive movement [1]. ATP binding to the nucleotide-free acto-MVS1 complex leads to acto-myosin dissociation. Once detached from

actin, ATP hydrolysis and subsequent rebinding to actin are very rapid, as is P_i release from the newly formed acto-myosin complex. The subsequent release of ADP however is slow and rate limiting. Interestingly, for this particular myosin, Mg^{2+} seems to be released prior to ADP, suggesting that free Mg^{2+} concentration may modulate myosin V's kinetics [22, 23]. The biochemical studies suggest that a single head spends ~70% of its kinetic cycle strongly bound to actin [1]. From this it can be estimated that a double-headed myosin V with stochastically and independently cycling heads would remain bound to actin for on average ~8 biochemical cycles before detaching with both heads [6]. Single molecule studies *in vitro*, however, have shown myosin V to be much more processive than this and to produce in the range of 10–60 steps per diffusional encounter with actin [7, 9, 12–14, 16, 18, 24, 25]. These studies suggest that the key to the increased processivity lies in a strain-dependent kinetic gating mechanism of the two heads.

2. Single molecule mechanical studies using optical tweezers

Optical tweezer based force transducers have been used extensively to study the motion and force produced by individual motor proteins. In the three-bead assay shown in figures 2 and 3 a single actin filament is suspended between two plastic beads (~1 μm diameter) held in two optical tweezers [26, 27]. The filament is positioned over a third, surface-bound glass microsphere, on which myosin molecules are immobilized at a low enough density to ensure mechanical interactions of single myosin molecules with actin occur. The positions of both beads holding the actin filament are recorded using two quadrant photodetectors [28, 29]. Myosin attachments to actin can be identified by the change in thermal noise of the signal, corresponding to sudden changes in system stiffness as myosin binds to actin (figure 3) [27]. The mean of the amplitudes of attachment events, measured relative to the mean rest position of the trapped beads, indicates the average displacement produced by a single myosin head interacting with actin. The spread of the distribution of displacements is explained by the randomizing effect of thermal motion on the binding positions for myosin along the thermally moving actin filament [27]. If the power spectral density of thermal noise is used as an indicator of system stiffness, the time resolution is usually ~10–15 ms in these experiments ($f_c = \kappa/(2\pi\beta) \sim 500$ Hz = roll-off frequency of the Lorentzian power density spectrum; $\kappa = 2\kappa_{trap} + \kappa_{add}$ is the system stiffness with κ_{trap} = trap stiffness (~0.02 pN nm^{-1}) and κ_{add} = additional stiffness due to myosin binding to actin; $\beta = 6\pi\eta r$, $r \sim 1.1$ μm = combined bead radii, and η = solution viscosity [29]). The time resolution can be improved using frequency filtering and analysis of the variance of the high frequency noise over smaller time windows [30, 31]. Alternatively, by applying a high frequency oscillation of e.g. 1 kHz to one of the optical tweezers, binding events can be detected within ~1 ms by monitoring the change in amplitude or phase of this signal transmitted to the bead in the stationary tweezers [32, 33]. Monitoring the amplitude using an analogue electronic detection circuit on-line, this signal has been used to feed back on the position of the tweezers, so that a range of loads can be applied very rapidly within ~2–3 ms after myosin binding to actin has been detected [32, 34].

Using this and related experimental designs [8, 13], it was shown that a processively moving myosin V molecule produces on average at least about ten successive steps per diffusional encounter with the filament track when moving against a low load of ~1 pN (figure 2). The step size is ~36 nm and processive movement is stalled at an opposing force of around 3 pN [10]. At loads in the range of ±2 pN the processive run length shows little load dependence [13]. This might enable myosin V to transport cargo efficiently against variable viscous drag forces through the cytoplasm. In simulations, cargo size and the elastic coiled coil connection between a bulky cargo and myosin V have been linked to the dynamics of

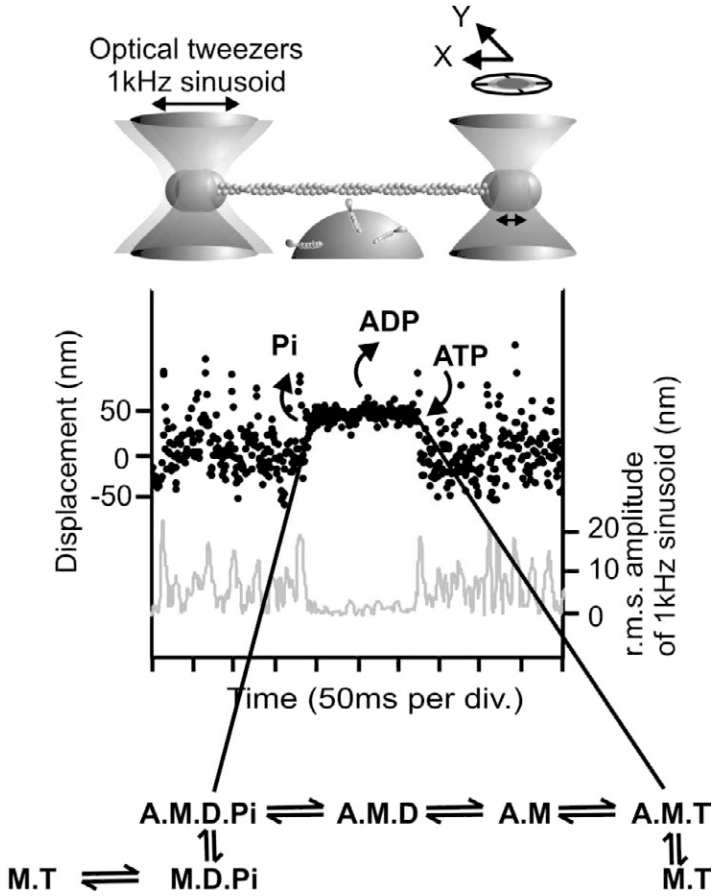

Figure 3. Single interactions of a myosin head with actin are identified by monitoring the amplitude of a 1 kHz carrier signal transmitted to the bead in the stationary tweezers (tweezers on the right). The record shows bead position measured in parallel to the actin filament axis versus time (black data points). The position of the laser tweezers on the left was oscillated at a frequency $f = 1$ kHz and amplitude $A_0 = 35$ nm rms in order to detect myosin binding with millisecond time resolution. The grey trace shows the transmission of this signal to the bead held in the stationary tweezers. The biochemical scheme indicates successive states in the acto-myosin interaction cycle.

processive movement through a viscous medium [35, 36]; the predictions from these studies, such as on regularity of the gait or velocity, still need to be tested in mechanical experiments. For forces close to stall (i.e. between 2 and 3 pN) and beyond, the kinetics of processive movement are strongly dependent on load and backward steps are observed with increasing frequency [6–8, 10, 13]. This suggests that there are load dependent transitions in myosin V's kinetic cycle, which could be associated with some biochemical transition and/or a load dependent diffusive component as the lead head searches out the next binding position along the actin filament [13].

Single headed myosin V constructs produced a working stroke of ∼20–25 nm, significantly shorter than the 36 nm step size produced by dimeric myosin V (figure 3) [6, 20]. This discrepancy implies that myosin V becomes internally strained when both heads are bound to actin. At low load and saturating ATP, the dwell times for single headed myosin V interactions with actin are two to three times longer than those between steps during processive runs by the

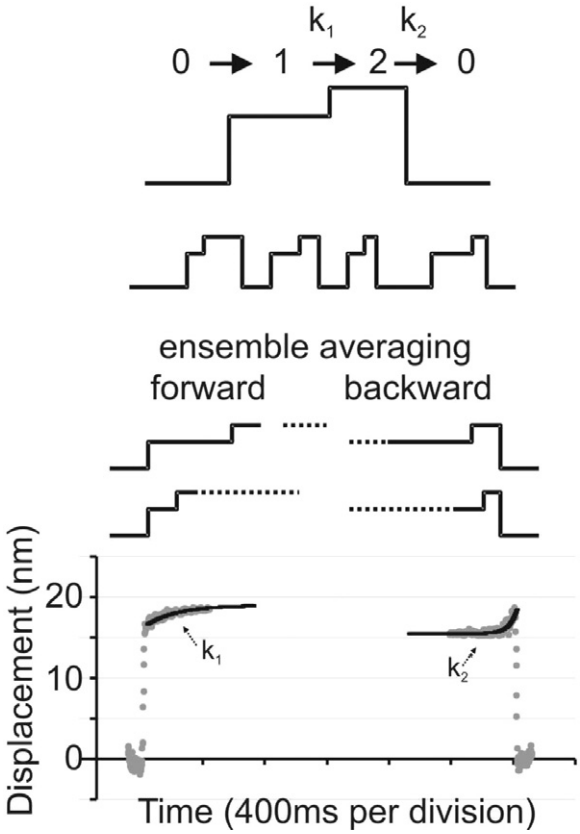

Figure 4. The two phases of the working stroke produced by a single myosin head can be resolved by an ensemble averaging technique. Binding events measured at 50 μM ATP were synchronized either to the time point of beginning or ending of each event and averaged (grey data points = averaged data) as illustrated in this cartoon. Amplitudes and transition rates of phase 1 and phase 2 of the working stroke (k_1 and k_2^*) were obtained by exponential fitting to the averaged data (solid black lines).

double-headed molecule [6]. This suggests that for the dimer, lead head binding might induce intramolecular strain that increases the rate of dissociation of the trailing head from actin [6, 8]. Such a load-dependent gaiting mechanism could serve to keep the biochemical cycles of both heads out of synchrony and increase the processive run length by reducing the probability that both heads detach from actin during the same time period. Knowing the kinetic properties of an individual head therefore may help to explain the processive movement of the dimeric molecule.

Detailed mechanical studies of the interaction of a single myosin V head with actin were recently performed under highly controlled load conditions. They revealed important insights into how load dependent kinetics may affect processivity of the dimeric motor (figures 3 and 4). Using an ensemble averaging method, binding events produced by a single myosin V head can be synchronized once to the time point of binding and once to the time point of detachment. The ensemble averages revealed that the working stroke produced by a single head occurs in two phases (figure 4) [6]. An initial displacement of ∼15 nm, probably concomitant with the binding of myosin.ADP.P_i to actin and subsequent P_i release, was produced within ∼1 ms of myosin binding. The kinetics of this initial displacement were too fast to be resolved in these

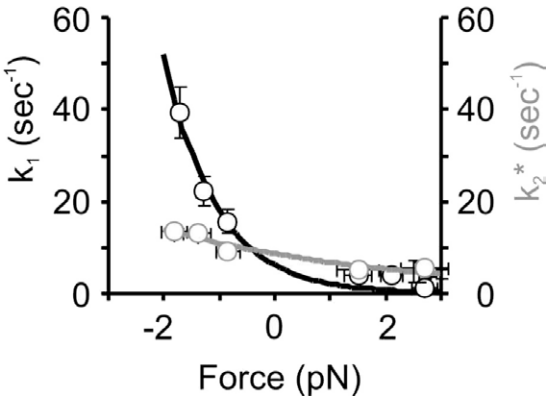

Figure 5. Load dependence of rates k_1 (in black) and k_2^* (in grey) at 3 μM ATP. The rates (circles) and exponential fits (solid lines) were obtained as described in the main text and in [6]. Essentially, binding events were ranked according to the individual load imposed on the acto-myosin complex during attachment and then grouped into six classes of load. k_1 and k_2^* were then fitted to the ensemble average of each class. Number of events per class was between 30 and 70. The plots could be fitted by single exponentials with $k_1 = k_{01}\exp(-Fd_1/k_bT)$ and $k_2^* = k_{02}^*\exp(-Fd_2/k_bT)$, with $k_{01} = 6\ s^{-1}$, $d_1 = 4.3$ nm, $k_{02}^* = 9\ s^{-1}$ and $d_2 = 0.9$ nm) as described in the main text. See also [6].

experiments. The subsequent dwell time was independent of ATP concentration and followed by a second displacement of ~5 nm with a transition rate constant, k_1, of ~5 s^{-1}, probably associated with ADP release. The following dwell time was ATP dependent with a transition rate constant, k_2, of ~1 $\mu M^{-1}\ s^{-1}$ ($k_2^* = k_2$ [ATP]), suggesting that myosin binding to actin is terminated when ATP binds to myosin, causing its detachment. The rate constants k_1 and k_2 determined in these mechanical experiments agree well with rates reported for ADP release and ATP binding in solution kinetic studies [1, 37]. Monitoring the amplitude of the 1 kHz carrier signal transmitted to the passive bead (figure 3) enables each myosin binding event to be detected within ~1–2 ms and a range of loads to be applied within ~3 ms to each newly formed acto-myosin complex [32]. Load was applied by moving the tweezers in the direction of the myosin working stroke or against it. The individual load experienced by each binding event was composed of the applied load (due to moving the tweezers following detection of binding), plus load caused by myosin binding to randomized positions along the actin filament, which moved thermally against the tweezers in between binding events [32]. The ensemble averaging approach was then applied to determine the effect of different loads on k_1 and k_2. It was found that the effect of a range of forces on k_1 could be described by a single exponential according to the Arrhenius transition state model with $k_1 = k_{01}e(-W/k_bT)$ (k_{01} = rate at zero load; $W = Fd_1$; F = load; distance parameter $d_1 = 4.3$ nm; thermal energy $k_bT \sim 4$ pN nm) (figure 5). The effect of the same range of forces on k_2^* could also be described by a single exponential with $k_2^* = k_{02}^*e(-W/k_bT)$ (k_{02}^* = rate at zero load; distance parameter $d_2 = 0.9$ nm) [34]. This suggests that there are at least two consecutive load dependent intervals during the lifetime of the acto-myosin complex, with the dwell time of the first interval particularly sensitive to load and probably terminated by ADP release.

One can also analyse the effect of load on the total lifetime of the acto-myosin complex. In figure 6 the reciprocal of the dwell time of individual acto-myosin binding events is plotted against the individual load experienced by each binding event. The plot was smoothed by averaging the lifetimes of events, ranked by load, over a running window of 40 events.

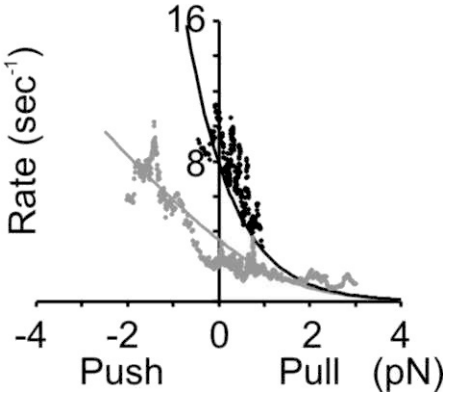

Figure 6. Effect of a range of forces on the detachment rate ($1/\text{lifetime}_{\text{overall}}$) s^{-1} at 3 μM (grey data points; 780 binding events) and 50 μM (black data points; 310 binding events) ATP. The binding events measured at the two different ATP concentrations were ranked by the load they experienced. The plots (1/lifetime versus load F) were smoothed by averaging over a running window of 40 events. The solid lines are calculated lifetimes assuming $k_{01} = 8.6\ s^{-1}$; $d_1 = 4.3$ nm; $k_{02} = 2\ \mu M^{-1}\ s^{-1}$; $d_2 = 0.9$ nm).

Figure 6 shows that the lifetimes become shorter when acto-myosin is pushed in the direction of the working stroke (detachment rates increase) while pulling increases the lifetimes. According to the biochemical scheme in figure 3 we expect the lifetime of the acto-myosin complex to comprise a series of biochemical states. However, solution kinetic data suggest that once myosin binds to actin, not only P_i release (>250 s^{-1} [1]) but also detachment of myosin from actin following binding of ATP (~850 s^{-1} [38]) is too fast to contribute considerably to the overall duration of the observed attached state (figure 3). If backward reaction rates are considered to be very small, each binding event can be described by two consecutive, irreversible transitions (figure 4), starting with myosin.ADP bound to actin and ending when ATP binds to the nucleotide-free acto-myosin complex (A.M.D $\xrightarrow{k1}$ A.M $\xrightarrow{k2}$ A.M.T). In this simplified model the mean lifetime of attachment, τ_{overall}, can then be described by the sum of two exponentially distributed dwell times described by k_1 and $k_2^* = k_2$ [ATP] (with $\tau_{\text{overall}} = \tau_1 + \tau_2 = 1/k_1 + 1/k_2^*$) and a probability density function $f(t) = k_1 k_2^*/(k_2^* - k_1)$ $(e^{-k1t} - e^{-k2^*t})$ (e.g. [8]). In figure 6 the reciprocal of the mean lifetime, $1/\tau_{\text{overall}}$, has been calculated as a function of force and ATP concentration, using rates k_{01} and k_{02} at zero load and distance parameters d_1 and d_2 as determined in figure 5 (with $\tau_{\text{overall}}(F) = 1/k_1(F) + 1/(k_2(F)\ [\text{ATP}]) = 1/(k_{01}e(-Fd_1/k_bT)) + 1/(k_{02}e(-Fd_2/k_bT)\ [\text{ATP}])$). Figure 6 shows that at low ATP concentrations the ATP dependent dwell time with little sensitivity towards load dominates the overall lifetime. At high ATP the overall lifetime is dominated by the strongly load dependent dwell time associated with ADP release. Calculated and experimental data agree well, supporting the idea that the total lifetime of the acto-myosin complex can be described by a model with two consecutive, load dependent dwell times. Another study, in which the effect of two different loads on the total lifetime of the acto-myosin complex was compared, confirmed shorter lifetimes for a pushing and longer ones for a pulling force of ~2 pN. Here, the effect of ATP and ADP concentrations on the lifetimes was consistent with a load dependent ADP state that seemed less sensitive for pushing than for pulling forces [39].

In order to develop a model to explain head coordination based on load dependent kinetics, we need to estimate the force acting on the lead and trail heads in the strained, two-head-

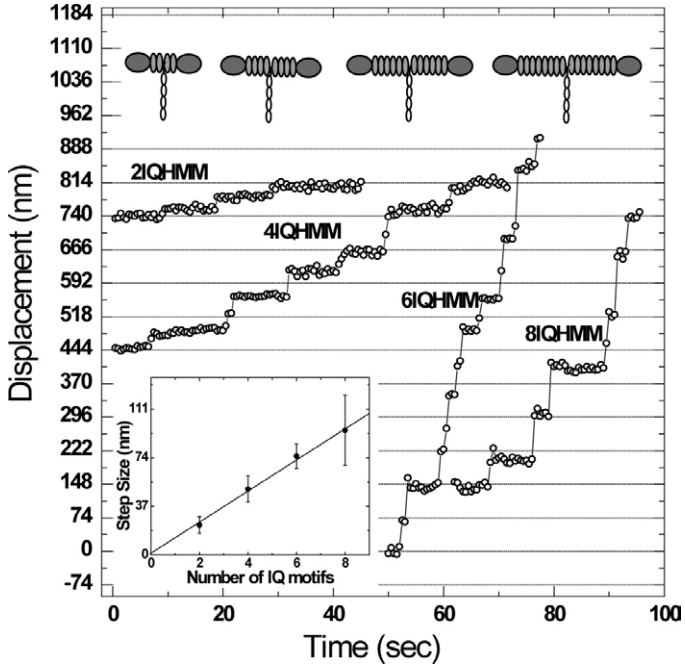

Figure 7. The step size is determined by the neck length. FIONA measurements of myosin V step size during processive runs for myosin V mutants with different neck lengths as determined by the number of light chain binding IQ motifs. The cartoons at the top depict each mutant. In this display the starting position of each processive run was arbitrarily picked for clarity reasons. The inset shows the mean step size for each mutant as a function of number of IQ motifs.

bound state. This force can be estimated knowing (1) the disparity between the size of the working stroke produced by a single head (∼20–25 nm) and the binding distance between the heads in the two-head-bound state (∼36 nm) and (2) the bending stiffness of myosin attached to actin ($\kappa_m \sim 0.2$ pN nm^{-1}) [6]. Depending on whether the lead head proceeds straight through its working stroke upon binding or not, the estimated force could reach upto ∼1.5 and 3.5 pN. With such a force acting in opposite directions on the lead and trail heads, we would expect the kinetics of ADP release to be accelerated on the trail and slowed down on the lead head respectively, increasing the probability of the trail head detaching first and reducing the chance of both heads detaching during the same time period, which would increase processivity. Another issue arising from the model of a strained two-head-bound state and a walking mechanism, based on a combination of a working stroke and a forward-biased diffusion of the free head, is how long it might take the free head to diffuse to the next binding position along actin, while building up intramolecular strain. While the diffusive reach of the free head is constrained by the attached head, the new binding position would be determined by the helical twist of the actin filament imposing a periodic free energy profile with minima at binding positions with lowest azimuthal distortion to the myosin V molecule along the actin helical pseudorepeat distance of 36 nm. The working stroke produced by the bound head would position the free head in an unstable region where diffusion is biased in the forward direction. Data obtained in an 'actin scanning' experiment are consistent with a simple model of a sinusoidal free energy landscape for the binding probability along each of the two intertwined actin protofilaments [6]. In this experiment an actin filament was moved back and forth past a

single myosin V head to probe whether binding occurred preferentially at specific sites along the actin filament. The derivative of the free-energy profile would give the diffusive force acting on an unbound myosin V head during processive movement, driving it forward by a distance of $d_x \sim 10$–16 nm to the next target actin monomer. One can calculate the average time it would take the unbound head to diffuse that distance as Kramers' first passage time [40, 41], $t_k = \tau\sqrt{(\pi/4)}\sqrt{(k_bT/U)}e(U/k_bT) \sim 0.1$ ms (the relaxation time of an unbound myosin V head in water is estimated to be $\tau = 6\pi\eta r/\kappa_m \sim 1$ μs; thermal energy $k_bT \sim 4$ pN nm; and the internal strain energy U calculated from κ_m is $U = (1/2)\kappa_m d_x^2 \sim 3k_bT$ [6]). This is only a very small fraction of the dwell at each processive step (~70 ms at saturating ATP concentrations [6, 8, 10]). However, with increasing load acting on the centre of mass of a processively moving myosin V, the distance d_x to be overcome by diffusion is expected to increase and t_k to rise respectively into the range of tens to hundreds of milliseconds. Intervals of reduced stiffness observed immediately before steps during processive movement might indicate this diffusive process [6].

3. Single molecule fluorescence studies

Single molecules of fluorescently labelled myosin V can be observed using total internal reflectance fluorescence (TIRF) microscopy. Two variations of TIRF microscopy have been used to provide evidence that myosin V moves in a hand-over-hand mechanism, whereby the two heads alternate leading and trailing positions. One involves a fluorescence technique termed FIONA, for 'fluorescent imaging with one nanometer accuracy'. If sufficient photons are collected the point spread function and thus the mean position of immobilized fluorophores can be determined at 1–2 nm resolution [14]. Myosin V molecules with a single cy3-labelled calmodulin (figure 7) [14, 16, 18] or GFP fused to the N-terminus of one head [18] can be observed to move stepwise under conditions of low ATP concentration, where the movement is slow enough to allow for collection of sufficient photons. The step size and kinetics of this movement is consistent with a hand-over-hand mechanism where the rear head moves forward the distance of one actin repeat (72 nm) as it becomes the new leading head. This distance is consistent with the step size of 36 nm found in the optical trapping experiments described above, which measure the movement of the centre of mass of the molecule. Even more direct evidence for a hand-over-hand mechanism came from FIONA studies where the two heads of a single myosin V molecule were differentially labelled with fluorophores of different colours. Alternating movements (72 nm) of the two heads could be seen and a constant 36 nm separation between the two attached heads was maintained [15, 17]. In a separate experiment, fluorescence polarization was used to determine the angles assumed by a fluorescent probe bound to calmodulin in the neck region of myosin V. When myosin V was moving processively alternating angles were observed that were consistent kinetically and structurally with a model in which the two heads were alternately moving in a hand-over-hand mechanism assuming the neck region was acting as a rigid lever arm [24].

The notion that the light chain binding region or neck of myosin might function as a lever arm that makes a large angle, rigid body motion about a pivot point in the motor domain was originally suggested by various myosin II crystal structures in different nucleotide states, which showed various positions of the neck region (see [42] for review). Negatively stained EM images of myosin V in the absence of actin also showed nucleotide-dependent lever-arm swings that corresponded to the pre- and post-power stroke angles seen in myosin V molecules bound to actin [21]. Myosin V lever-arm swings were directly observed by fast AFM imaging of myosin V in the presence of nucleotide [43]. Myosin V crystallography and combined cryo-EM of myosin-bound actin filaments with the docking of crystal structures into three-dimensional

reconstructions suggest that small movements of motor domain elements that occur in response to nucleotide binding and hydrolysis are transmitted through a transduction pathway to allow the neck region of myosin V to swing as much as ∼75°–105°, corresponding to a displacement of the tip of the lever arm of 20–36 nm [19, 44–46]. Strong support for the light chain binding region as a mechanical lever has come from a number of experiments where the neck region of myosin V has been either elongated or truncated by the addition or subtraction of IQ motifs, changing the mechanics of the motor [9, 16, 47, 48]. It was shown that the speed of actin filament movement over immobilized myosin heads on a surface, the speed of single myosin V molecules moving along immobilized actin filaments, the size of the power-stroke produced by a single myosin V head, and the step-size in processive runs of dimeric myosin V (figure 7) all varied roughly linearly with the length of the myosin V lever arm.

Myosin V molecules with two, four, six, or eight IQ motifs could all move processively [9, 16, 39, 47]. Given that molecules with fewer or more than six IQ motifs take smaller or larger than 36 nm steps, it is likely that these molecules spiral around the actin filament while moving. Purcell *et al* [9] reported that a two-headed myosin V fragment with only one IQ motif did not move processively in the single molecule mechanical experiment, but Tanaka *et al* [11] found that a chimera containing the myosin V head with one IQ motif fused to the rod domain of smooth muscle myosin could take two or three successive 36 nm steps.

The detailed biochemical and kinetic experiments described above used mouse or chicken myosin Va, but processivity is not a universal feature of class V myosins. ADP release is not rate limiting in the kinetic scheme of *Drosophila* myosin V and the molecule is not capable of moving actin filaments in a processive manner in motility assays [49]. In addition, it was concluded that the two type V myosins from *S. cerevisiae*, myo2p and myo4p, are not processive either [50]. Interestingly, however, if the motor domains of mouse myosin V are replaced by the motor domains of yeast myosin V, the chimaeric molecule is processive [51].

4. Models for processive movements

A number of models have been presented for the processive movement of myosin V, nearly all of which assume that the two-headed structure is necessary (an alternative model has been suggested in [52]). The nucleotide state and actin affinity of the two heads of myosin during dwell periods in between processive steps (figure 1) remain critical but unresolved issues. Stiffness measurements of the acto-myosin complex during processive movement detected a reduced level of stiffness just prior to each step transition [6]. This suggests that, at saturating ATP concentrations and low load, the molecule dwells mostly with both heads strongly bound to actin (states B or C in figure 1). This idea is consistent with biochemical, mechanical and structural studies suggesting that, under these conditions, myosin V dwells with both heads strongly bound in some ADP state(s) and that the detachment kinetics of the trail and lead heads are determined by accelerated and reduced ADP release respectively, due to intramolecular strain [6, 8, 34, 37, 39]. According to this model myosin V moves processively as long as the lead head rebinds strongly to actin before the trail head releases ADP and subsequently binds ATP, resulting in detachment of that head and, thus, the whole molecule. Unresolved issues are whether the lead head can produce its working stroke while the trail head is still bound and also the coupling between conformational changes observed in the mechanical studies and ADP, P_i release or isomerization processes.

Models derived from fitting the nucleotide dependence of run length and velocity of mouse myosin V suggest differences from the above mode. First, the dwell state is dominated by a molecule with ADP in the strongly bound rear head and ADP.P_i in the weakly bound lead head, and second, termination of a processive run occurs most commonly from this same

state [25]. Starting in this state, two stepping pathways are proposed. In the first, the lead head attaches strongly and releases its phosphate, resulting in two ADP-bound heads attached to actin (figure 1 state B) as in the model above. In the second, the trail releases ADP while the lead head is still weakly bound. In both pathways continuation of processive movement will be determined by strong attachment of the lead head, coupled to P_i release, before the attached trailing head releases ADP. The effect of differences in species and assay conditions must be explored.

5. Conclusions

Myosin V mutagenesis is well advanced and enables both *in vivo* and *in vitro* studies. Because of its large size single molecule imaging techniques have been successfully applied to study the motor in the presence and absence of its binding partners. Its kinetics and many of its mechanical properties have been elucidated in a series of elegant solution kinetic and single molecule mechanical and fluorescence experiments. Stochastic models, interpreting measured force–velocity relationships and relating these to kinetics and substeps of load dependent forward and backward reactions, can now be tested [53]. First steps in combining single molecule and fluorescence measurements reporting nucleotide binding have been made [54], and progress in this field will help to develop new and validate existing models addressing head coordination and step-size distributions in myosin V [55, 56]. They will provide complementary information to structural studies, for example on the light chain binding domain of myosin V, assumed by many to act as a lever arm [57]. Myosin V is an ideal molecule to study the molecular basis of processivity, and dissecting its molecular mechanism will contribute to a better understanding of force generation in other myosins and molecular motors in general.

Acknowledgments

We would like to thank NIH, MRC and IRC Bionanotechnology for financial support.

References

[1] De La Cruz E M, Wells A L, Rosenfeld S S, Ostap E M and Sweeney H L 1999 The kinetic mechanism of myosin V *Proc. Natl Acad. Sci. USA* **96** 13726–31
[2] Wu X F S, Rao K, Zhang H, Wang F, Sellers J R, Matesic L E, Copeland N G, Jenkins N A and Hammer J A 2002 Identification of an organelle receptor for myosin-Va *Nat. Cell Biol.* **4** 271–8
[3] Fukuda M, Kuroda T S and Mikoshiba K 2002 Slac2-a/melanophilin, the missing link between Rab27 and myosin Va—Implications of a tripartite protein complex for melanosome transport *J. Biol. Chem.* **277** 12432–6
[4] Provance D W, James T L and Mercer J A 2002 Melanophilin, the product of the leaden locus, is required for targeting of myosin-Va to melanosomes *Traffic* **3** 124–32
[5] Wang F, Thirumurugan K, Stafford W F, Hammer J A, Knight P J and Sellers J R 2004 Regulated conformation of myosin V *J. Biol. Chem.* **279** 2333–6
[6] Veigel C, Wang F, Bartoo M L, Sellers J R and Molloy J E 2002 The gated gait of the processive molecular motor, myosin V *Nat. Cell Biol.* **4** 59–65
[7] Uemura S, Higuchi H, Olivares A O, De La Cruz E M and Ishiwata S 2004 Mechanochemical coupling of two substeps in a single myosin V motor *Nat. Struct. Mol. Biol.* **11** 877–83
[8] Rief M, Rock R S, Mehta A D, Mooseker M S, Cheney R E and Spudich J A 2000 Myosin-V stepping kinetics: A molecular model for processivity *Proc. Natl Acad. Sci. USA* **97** 9482–6
[9] Purcell T J, Morris C, Spudich J A and Sweeney H L 2002 Role of the lever arm in the processive stepping of myosin V *Proc. Natl Acad. Sci. USA* **99** 14159–64

[10] Mehta A D, Rock R S, Rief M, Spudich J A, Mooseker M S and Cheney R E 1999 Myosin-V is a processive actin-based motor *Nature* **400** 590–3
[11] Tanaka H, Homma K, Iwane A H, Katayama E, Ikebe R, Saito J, Yanagida T and Ikebe M 2002 The motor domain determines the large step of myosin-V *Nature* **415** 192–5
[12] Ali M Y, Uemura S, Adachi K, Itoh H, Kinosita K and Ishiwata S 2002 Myosin V is a left-handed spiral motor on the right-handed actin helix *Nat. Struct. Biol.* **9** 464–7
[13] Clemen A E M, Vilfan M, Jaud J, Zhang J S, Barmann M and Rief M 2005 Force-dependent stepping kinetics of myosin-V *Biophys. J.* **88** 4402–10
[14] Yildiz A, Forkey J N, McKinney S A, Ha T, Goldman Y E and Selvin P R 2003 Myosin V walks hand-over-hand: Single fluorophore imaging with 1.5-nm localization *Science* **300** 2061–5
[15] Warshaw D M, Kennedy G G, Work S S, Krementsova E B, Beck S and Trybus K M 2005 Differential labeling of myosin V heads with quantum dots allows direct visualization of hand-over-hand processivity *Biophys. J.* **88** L30–2
[16] Sakamoto T, Yildez A, Selvin P R and Sellers J R 2005 Step-size is determined by neck length in myosin V *Biochemistry* **44** 16203–10
[17] Churchman L S, Okten Z, Rock R S, Dawson J F and Spudich J A 2005 Single molecule high-resolution colocalization of Cy3 and Cy5 attached to macromolecules measures intramolecular distances through time *Proc. Natl Acad. Sci. USA* **102** 1419–23
[18] Snyder G E, Sakamoto T, Hammer J A, Sellers J R and Selvin P R 2004 Nanometer localization of single green fluorescent proteins: Evidence that myosin V walks hand-over-hand via telemark configuration *Biophys. J.* **87** 1776–83
[19] Walker M L, Burgess S A, Sellers J R, Wang F, Hammer J A, Trinick J and Knight P J 2000 Two-headed binding of a processive myosin to F-actin *Nature* **405** 804-+
[20] Moore J R, Krementsova E B, Trybus K M and Warshaw D M 2001 Myosin V exhibits a high duty cycle and large unitary displacement *J. Cell Biol.* **155** 625–35
[21] Burgess S, Walker M, Wang F, Seller J R, White H D, Knight P J and Trinick J 2002 The prepower stroke conformation of myosin V *J. Cell Biol.* **159** 983–91
[22] Hannemann D E, Cao W X, Olivares A O, Robblee J P and De La Cruz E M 2005 Magnesium, ADP, and actin binding linkage of myosin V: Evidence for multiple myosin V-ADP and actomyosin V-ADP states *Biochemistry* **44** 8826–40
[23] Rosenfeld S S, Houdusse A and Sweeney H L 2005 Magnesium regulates ADP dissociation from myosin V *J. Biol. Chem.* **280** 6072–9
[24] Forkey J N, Quinlan M E, Shaw M A, Corrie J E T and Goldman Y E 2003 Three-dimensional structural dynamics of myosin V by single-molecule fluorescence polarization *Nature* **422** 399–404
[25] Baker J E, Krementsova E B, Kennedy G G, Armstrong A, Trybus K M and Warshaw D M 2004 Myosin V processivity: Multiple kinetic pathways for head-to-head coordination *Proc. Natl Acad. Sci. USA* **101** 5542–6
[26] Finer J T, Simmons R M and Spudich J A 1994 Single myosin molecule mechanics-piconewton forces and nanometer steps *Nature* **368** 113–9
[27] Molloy J E, Burns J E, Kendrickjones J, Tregear R T and White D C S 1995 Movement and force produced by a single myosin head *Nature* **378** 209–12
[28] Mehta A D, Finer J T and Spudich J A 1997 Detection of single-molecule interactions using correlated thermal diffusion *Proc. Natl Acad. Sci. USA* **94** 7927–31
[29] Veigel C, Bartoo M L, White D C S, Sparrow J C and Molloy J E 1998 The stiffness of rabbit skeletal actomyosin cross-bridges determined with an optical tweezers transducer *Biophys. J.* **75** 1424–38
[30] Smith D A, Steffen W, Simmons R M and Sleep J 2001 Hidden-Markov methods for the analysis of single-molecule actomyosin displacement data: The variance-hidden-Markov method *Biophys. J.* **81** 2795–816
[31] Capitanio M, Canepari M, Cacciafesta P, Lombardi V, Cicchi R, Maffei M, Pavone F S and Bottinelli R 2006 Two independent mechanical events in the interaction cycle of skeletal muscle myosin with actin *Proc. Natl Acad. Sci. USA* **103** 87–92
[32] Veigel C, Molloy J E, Schmitz S and Kendrick-Jones J 2003 Load-dependent kinetics of force production by smooth muscle myosin measured with optical tweezers *Nat. Cell Biol.* **5** 980–6
[33] Veigel C, Coluccio L M, Jontes J D, Sparrow J C, Milligan R A and Molloy J E 1999 The motor protein myosin-I produces its working stroke in two steps *Nature* **398** 530–3
[34] Veigel C, Schmitz S, Wang F and Sellers J R 2005 Load-dependent kinetics of myosin-V can explain its high processivity *Nat. Cell Biol.* **7** 861–9
[35] Schilstra M J and Martin S R 2006 An elastically tethered viscous load imposes a regular gait on the motion of myosin-V. Simulation of the effect of transient force relaxation on a stochastic process *J. R. Soc. Interface* **3** 153–65

[36] Zeldovich K B, Joanny J F and Prost J 2005 Motor proteins transporting cargos *Eur. Phys. J.* E **17** 155–63
[37] Rosenfeld S S and Sweeney H L 2004 A model of myosin V processivity *J. Biol. Chem.* **279** 40100–11
[38] Trybus K M, Krementsova E and Freyzon Y 1999 Kinetic characterization of a monomeric unconventional myosin V construct *J. Biol. Chem.* **274** 27448–56
[39] Purcell T J, Sweeney H L and Spudich J A 2005 A force-dependent state controls the coordination of processive myosin V *Proc. Natl Acad. Sci. USA* **102** 13873–8
[40] Howard J 2001 *Mechanics of Motor Proteins and the Cytoskeleton* (Sunderland, MA: Sinauer Associates)
[41] Kramers H A 1940 Brownian motion in a field of force and the diffusion model of chemical reactions *Physica* **7** 284–304
[42] Holmes K C and Geeves M A 2000 The structural basis of muscle contraction *Phil. Trans. R. Soc.* B **355** 419–31
[43] Ando T, Kodera N, Takai E, Maruyama D, Saito K and Toda A 2001 A high-speed atomic force microscope for studying biological macromolecules *Proc. Natl Acad. Sci. USA* **98** 12468–72
[44] Coureux P D, Sweeney H L and Houdusse A 2004 Three myosin V structures delineate essential features of chemo-mechanical transduction *EMBO J.* **23** 4527–37
[45] Volkmann N, Liu H J, Hazelwood L, Krementsova E B, Lowey S, Trybus K M and Hanein D 2005 The structural basis of myosin V processive movement as revealed by electron cryomicroscopy *Mol. Cell* **19** 595–605
[46] Coureux P D, Wells A L, Menetry J, Yengo C M, Morris C A, Sweeney H L and Houdusse A 2003 A structural state of the myosin V motor without bound nucleotide *Nature* **425** 419–23
[47] Sakamoto T, Wang F, Schmitz S, Xu Y H, Xu Q, Molloy J E, Veigel C and Sellers J R 2003 Neck length and processivity of myosin V *J. Biol. Chem.* **278** 29201–7
[48] Moore J R, Krementsova E B, Trybus K M and Warshaw D M 2004 Does the myosin V neck region act as a lever? *J. Muscle Res. Cell Motility* **25** 29–35
[49] Toth J, Kovacs M, Wang F, Nyitray L and Sellers J R 2005 Myosin V from drosophila reveals diversity of motor mechanisms within the myosin V family *J. Biol. Chem.* **280** 30594–603
[50] Reck-Peterson S L, Tyska M J, Novick P J and Mooseker M S 2001 The yeast class V myosins, Myo2p and Myo4p, are nonprocessive actin-based motors *J. Cell Biol.* **153** 1121–6
[51] Krementsova E B, Hodges A R, Lu H and Trybus K M 2006 Processivity of chimeric class V myosins *J. Biol. Chem.* **281** 6079–86
[52] Watanabe T M, Tanaka H, Iwane A H, Maki-Yonekura S, Homma K, Inoue A, Ikebe R, Yanagida T and Ikebe M 2004 A one-headed class V myosin molecule develops multiple large (approximate to 32 nm) steps successively *Proc. Natl Acad. Sci. USA* **101** 9630–5
[53] Kolomeisky A B and Fisher M E 2003 A simple kinetic model describes the processivity of myosin-V *Biophys. J.* **84** 1642–50
[54] Ishijima A, Kojima H, Funatsu T, Tokunaga M, Higuchi H, Tanaka H and Yanagida T 1998 Simultaneous observation of individual ATPase and mechanical events by a single myosin molecule during interaction with actin *Cell* **92** 161–71
[55] Vilfan A 2005 Elastic lever-arm model for myosin V *Biophys. J.* **88** 3792–805
[56] Lan G H and Sun S X 2005 Dynamics of myosin-V processivity *Biophys. J.* **88** 999–1008
[57] Terrak M, Rebowski G, Lu R C, Grabarek Z and Dominguez R 2005 Structure of the light chain-binding domain of myosin V *Proc. Natl Acad. Sci. USA* **102** 12718–23